Journal of Structural Geology, Vol. 2, No. 1/2, pp. 83 to 99.
Pergamon Press Ltd. 1980. Printed in Great Britain.

0191-8141/80/0601-0083 $02.00/0

Shear zone geometry: a review

J. G. RAMSAY

Geologisches Institut, ETH, CH-8092 Zürich, Switzerland

(Received 26 June 1979; accepted in revised form 26 September 1979)

Abstract—Shear zones may be classified into brittle, brittle–ductile, and ductile shear zones. The geometry and displacement boundary conditions of these zones are established. The geometric characteristics of ductile shear zones relevant to geological studies are described: orientations and values of principal finite strains, rotation, and deformation features of pre-existing planar and linear structures. Ductile shear zones show a fabric (schistosity and lineation) related to the finite strain state. The methods for determining strains and displacements from field studies are described.

Shear zones commonly occur in conjugate sets, but the two differently oriented sets do not seem to be able to operate synchronously. The angular relationships of conjugate ductile shear zones are different from those of brittle shear zones.

The termination of all types of shear zones poses complex compatibility problems, some solutions are suggested.

A synthesis of shear zone geometry in regions of crustal contraction and crustal extensions is made, and ideas on how deep level ductile shear zones relate to high level brittle shears and gliding nappes are put forward.

TYPES OF SHEAR ZONES

GENERATIONS of geologists studying the natural deformations of the Earth's crust have noticed that high deformations are often localised in narrow, sub-parallel sided zones, and those have been loosely termed *shear zones*.

Faults or *brittle shear zones* are special varieties of shear zones, where a clear discontinuity exists between the sides of the zone, and where the shear zone walls are almost unstrained or perhaps brecciated (Fig. 1a). Such fault zones are generally attributed to brittle failure controlled by the limiting elastic properties of the rock under orogenic stress. Other fault-like features show some ductile deformation in the walls, and are perhaps best termed *brittle–ductile shear zones*. The walls may show permanent strain for a distance of up to 10 metres on either side of the fault break (Fig. 1b). In the past these distortions have often been attributed to localised drag effects as the adjacent walls of the fault moved past each other, and the distortion of marker layers of rock entering this zone of flow have been used to determine the approximate movement sense of the displacement vector. This latter deduction is not always possible, because the geometry of the deflected marker surfaces in this zone is controlled by the line of intersection of the initial surface and the shear zone, and not by the movement vector. In brittle–ductile shear zones it is quite possible that the ductile part of the deformation history formed at a different time from that of the fault discontinuity. Another type of brittle–ductile shear zone is the extension failure of extension openings, usually filled with fibrous crystalline material, the openings generally making an angle of 30° or more with the shear zone and sometimes showing a sigmoidal form. The rock material between the extension fissures generally shows a certain amount of coherent permanent deformation, and it appears that the extension fissures developed at some stage of the deformation when a certain limit to coherent flow in the zone was reached. The third type of shear deformation is that of the *ductile shear zone*. Here the deformation and differential displacement of the walls is accomplished entirely by ductile flow, and on the scale of the rock outcrop no discontinuites can be seen (Fig. 1d). Marker layers in the country rock can be traced through the shear zone, they are deflected and may change their thickness, but they remain unbroken. Ductile shear zones are extremely common in deformed crystalline basement rocks (granites, gabbros, gneisses) which have been deformed under metamorphic conditions of greenschist, blueschist, amphibolite and granulite facies. They seem to be the dominant deformation mode whereby large masses of physically rather homogeneous rock can change shape under medium to high grades of metamorphism. The mineralogy of the rock in the ductile shear zone usually shows the characteristics of the metamorphic facies under which it developed. It is historically interesting as well as pertinent to this last point to note that the first understanding of the geological significance of hornblende schist was made from a study of shear zones in the Lewisian rocks of NW Scotland by Teall (1885). He was able to trace an unmetamorphosed basaltic dyke with normal igneous mineralogy though an amphibolite grade shear zone,

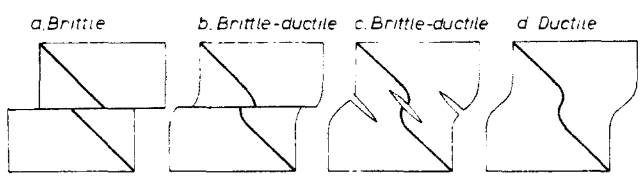

Fig. 1. Types of shear zones.

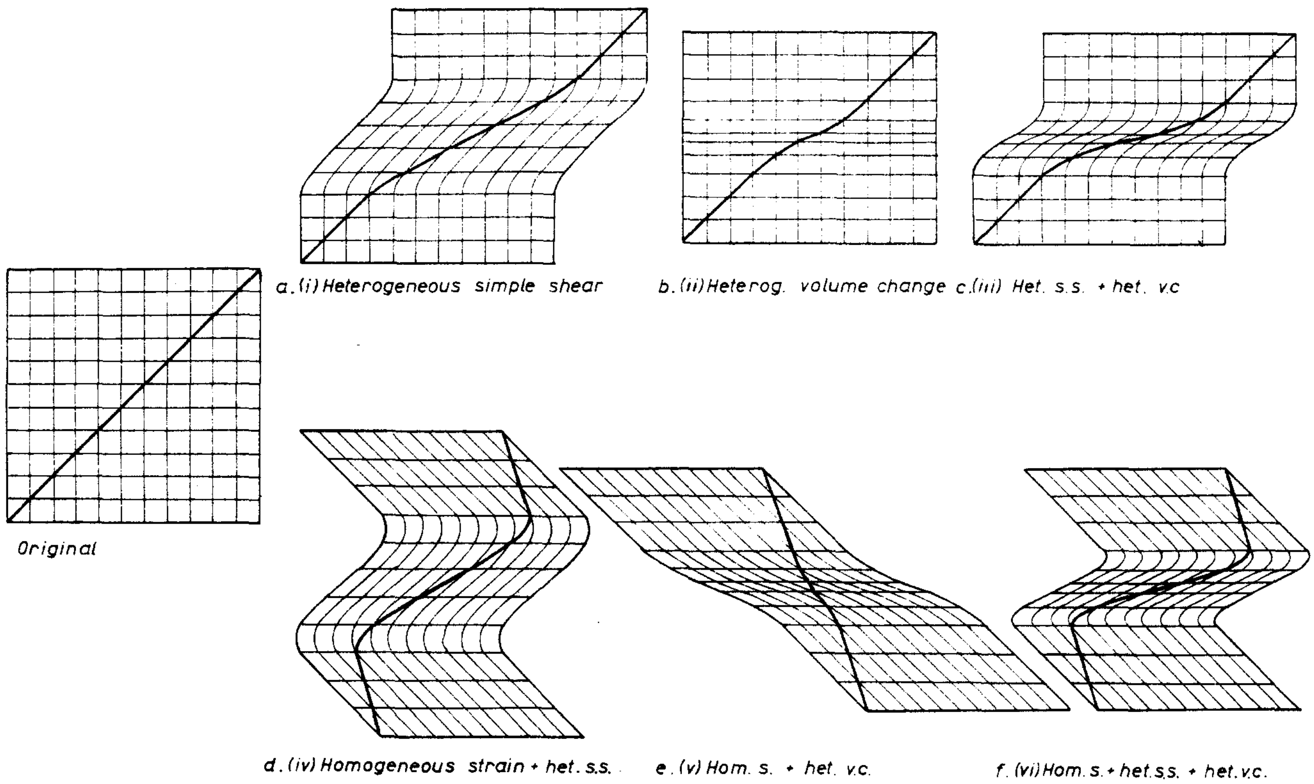

Fig. 3. Displacement fields of ductile shear zones.

where it was transformed, into a hornblende-biotite–oligoclase rock with a strongly schistose fabric.

The main aim of this contribution is to establish the geometrical features of shear zones, especially those of the ductile and brittle–ductile varieties, because in many regions these seem to be the deep level counterparts of brittle shear zones and faults seen at higher levels in the crust. Examples of these various types of shear zones are illustrated in Fig. 2.

SHEAR ZONE GEOMETRY

The boundary conditions for the geometrically simplest shear zones are first, that the shear zone is parallel sided, and second, that the displacement profiles along any cross sections of the zone are identical. This second condition implies that the finite strain profiles and the orientations and characteristic geometric features of small scale structural features across profiles are also identical — these being more easily recognised boundary conditions in practical geological terms. Although these conditions can never be completely realistic because all shear zones have to come to an end (their sides must eventually come together or splay apart, and their displacement profiles must change near their termination), it is my experience that very many shear zones often approximate closely to these over quite large zone lengths.

From the nature of the general displacement equations it can be shown that these boundary conditions constrain the types of displacement field (Ramsay & Graham 1970, pp. 796–798). If the walls of the shear zone are unstrained, then the following displacement fields are possible:

(i) heterogeneous simple shear (Fig. 3a);
(ii) heterogeneous volume change (Fig. 3b);
(iii) combinations of (ii) and (i) (Fig. 3c).

For the mathematical description of the third of these possibilities one should note that the order of the simple shear and volume change components should be specified. In this paper the simple shear component is followed by a volume reduction even though the two effects may have been geologically synchronous. This choice leads to mathematically simpler equations than when the two effects are reversed. In all three types the intermediate or Y_f axis of the finite strain ellipsoid (axes

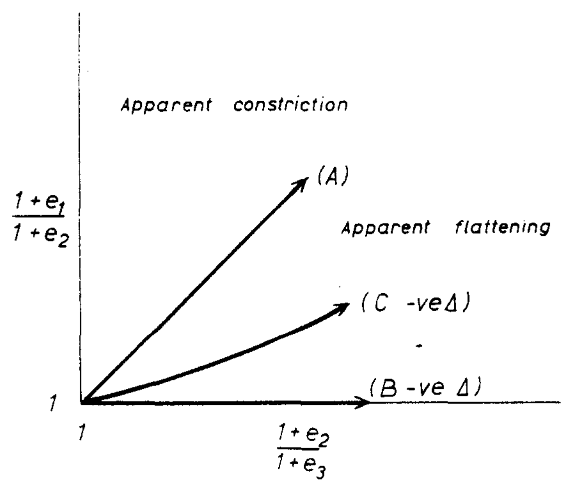

Fig. 4. Strain fields of the ductile shear zones of types (i), (ii), and (iii) shown in Fig. 3.

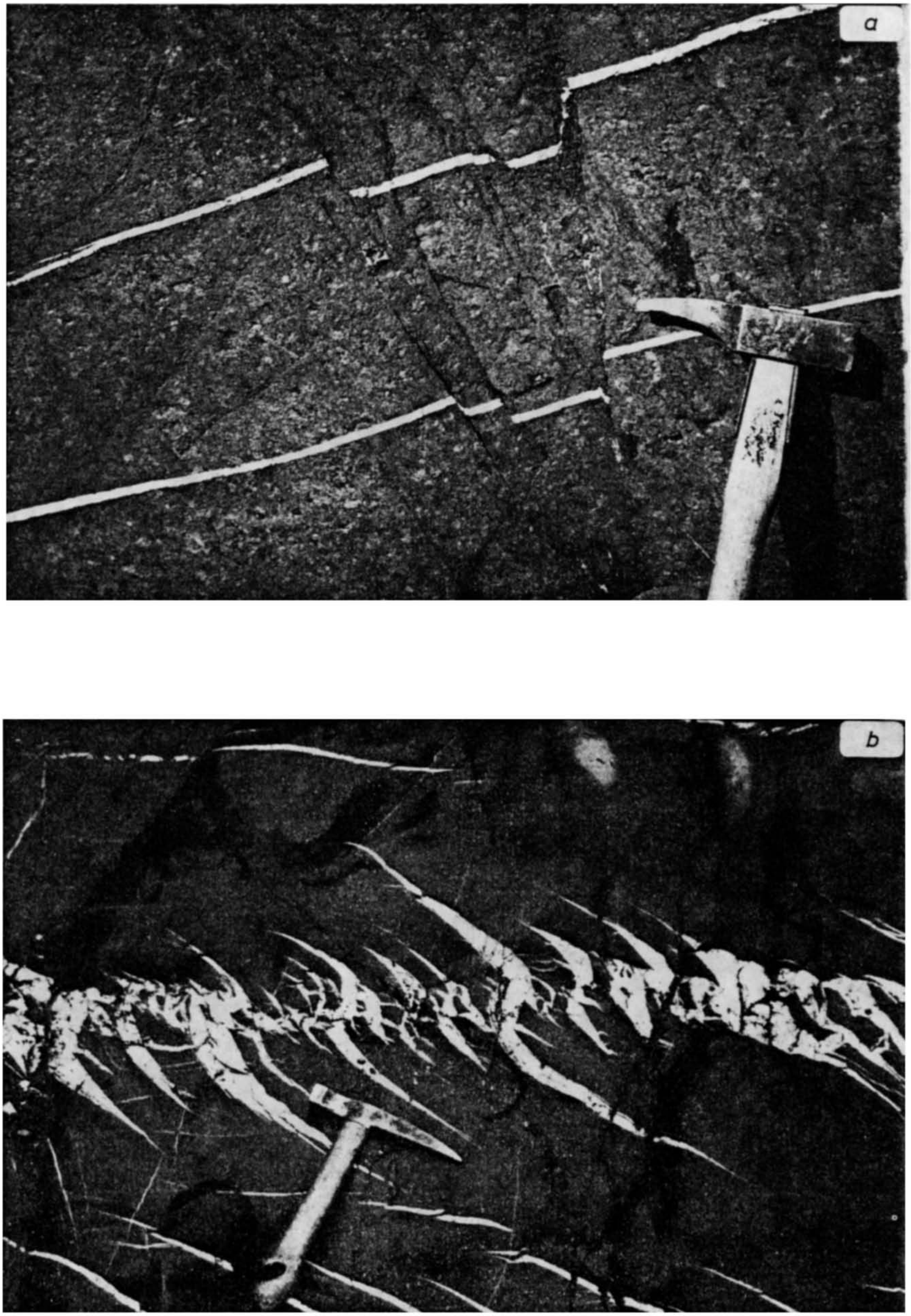

Fig. 2 (a) and (b). For caption see p. 87

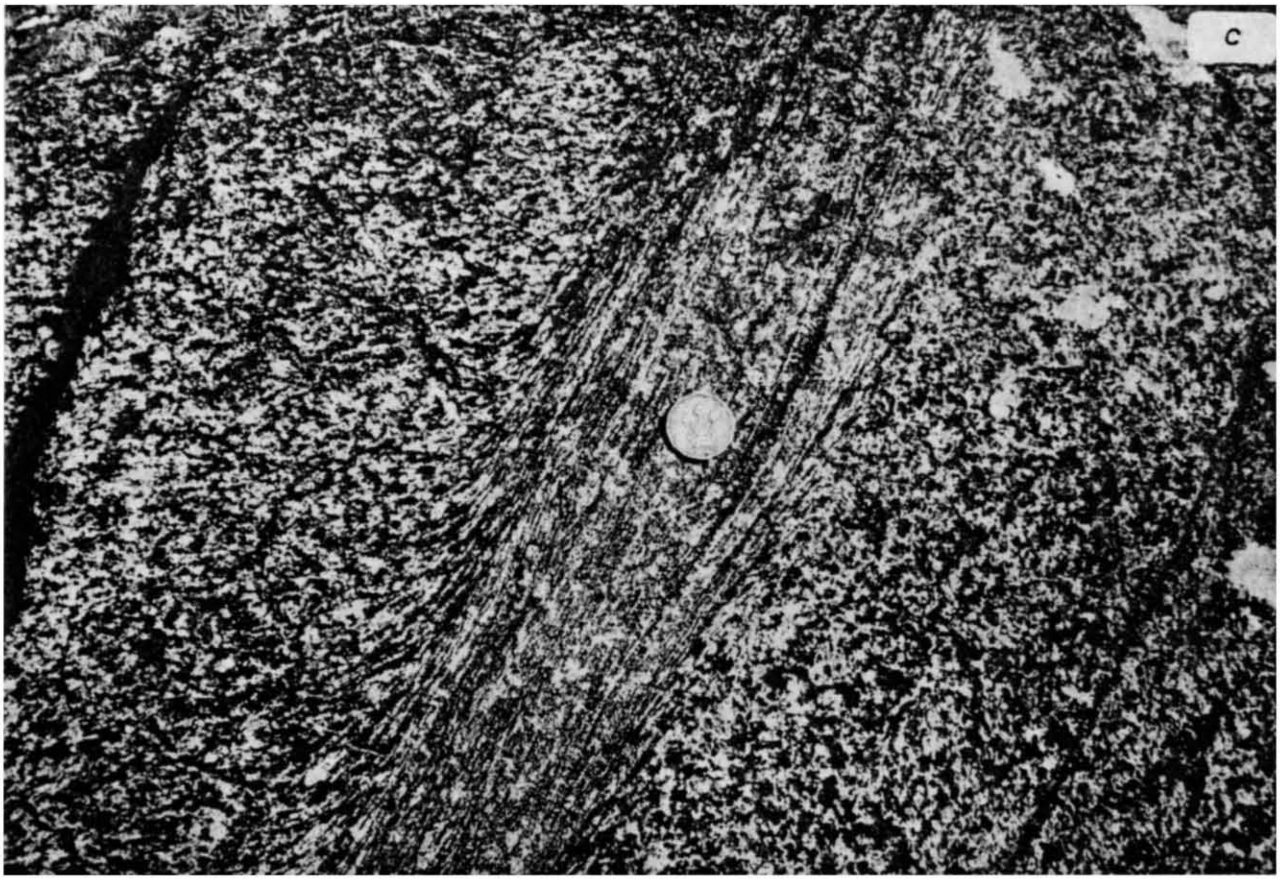

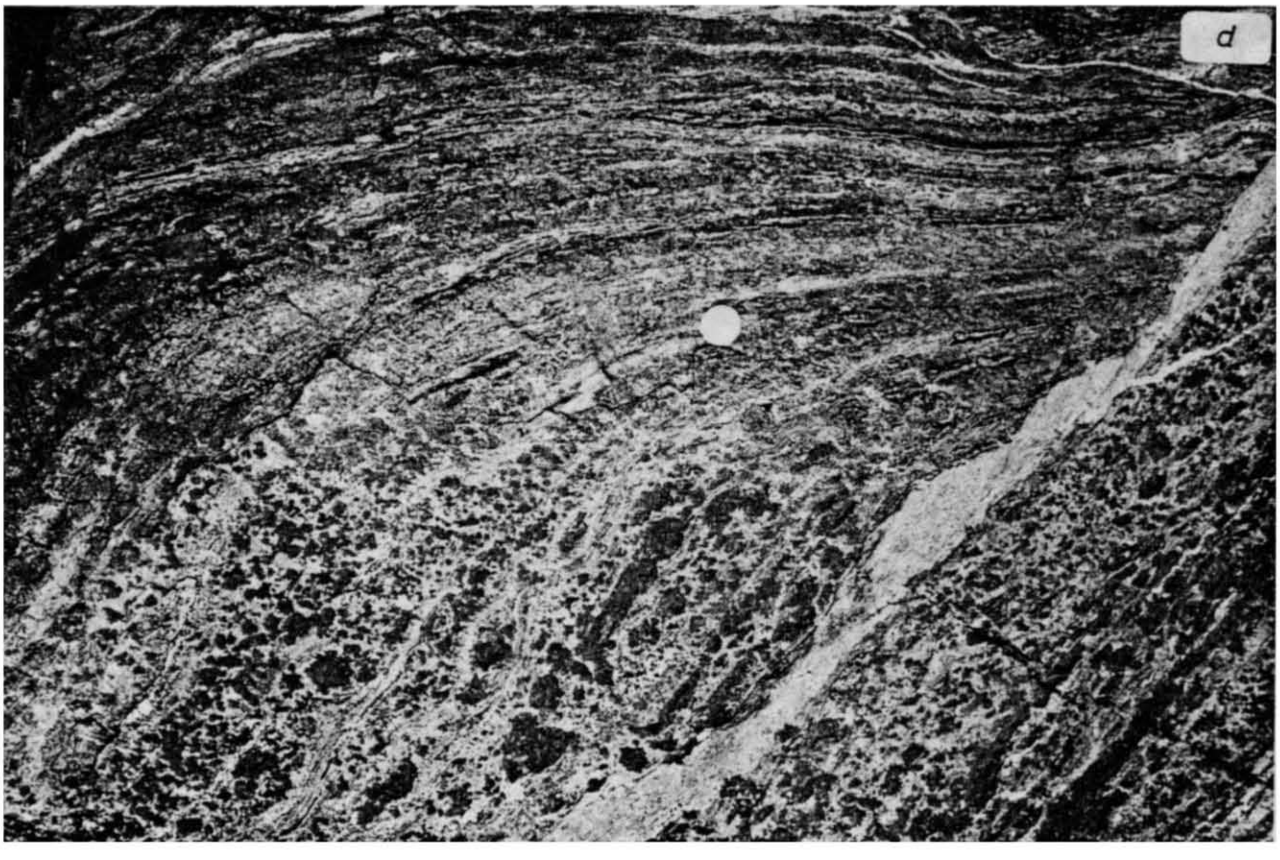

Fig. 2 (c) and (d). For caption see p. 87

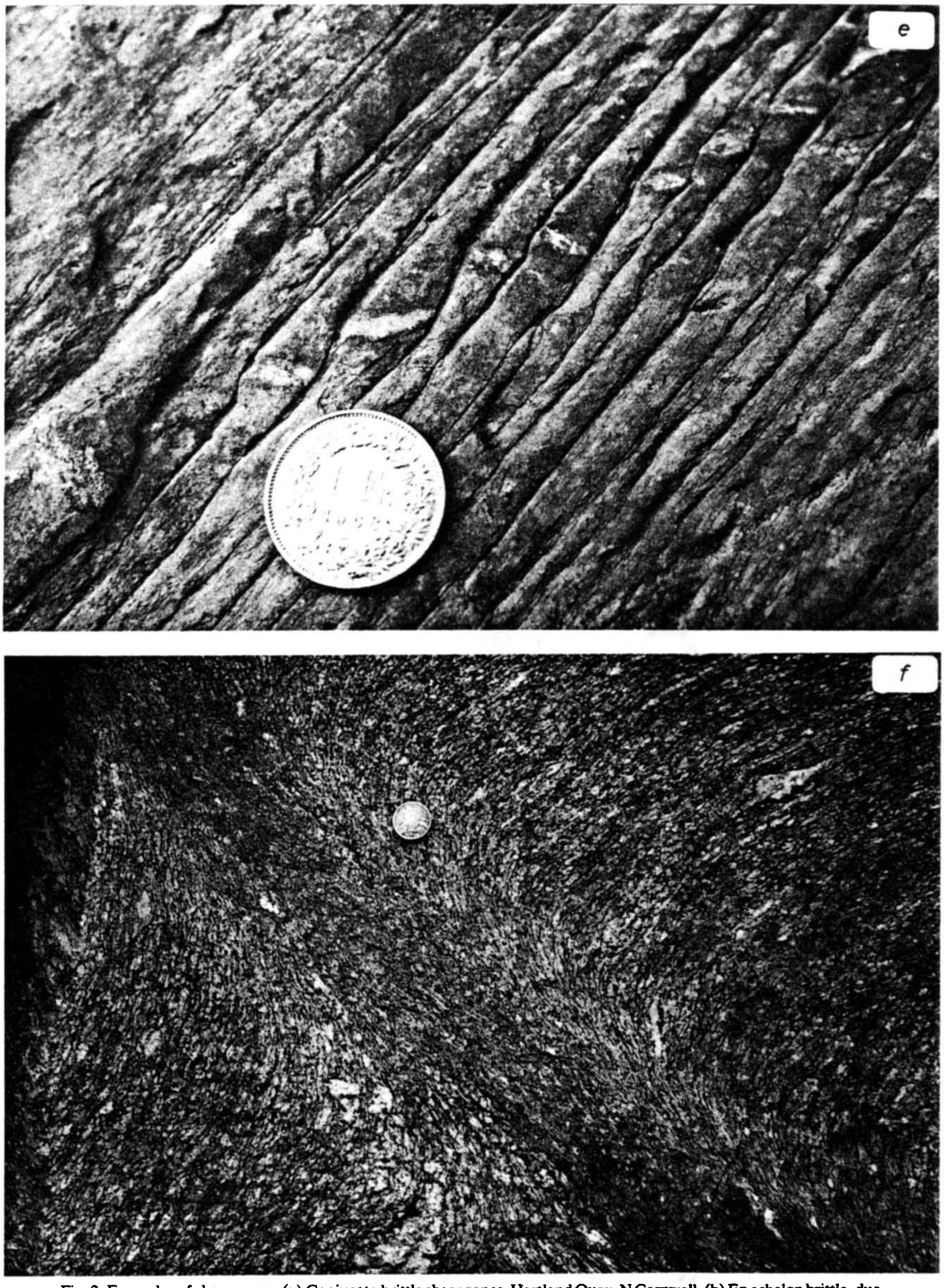

Fig. 2. Examples of shear zones. (a) Conjugate brittle shear zones, Hartland Quay, N Cornwall. (b) En echelon brittle–ductile shear zone; quartz filled vein fissures in a sandstone, Millook Haven, N Cornwall. (c) Ductile shear zone in Lewisian metagabbro, Castell Odair, N. Uist, Scotland. (d) Ductile shear zone in granulitic gneiss, showing modifications of mineralogy, N. Uist, Scotland. The wall of the shear zone shows dark garnet with orthopyroxenes, and this is transformed into amphibolite facies mineralogy (hornblende, biotite, clinopyroxene) inside the shear zone (e) Shear zones with volume reduction zones in Jurassic limestone, Gasterntal, Central Switzerland. (f) Ductile shear zones with deformed matrix gneisses, Cristallina, Ticino, central Switzerland.

Fig. 10. (a) Sigmoidal schistosity fabric produced in a ductile shear zone. (b) Strained xenoliths in a shear zone cutting granitic rocks. Laghetti, Ticino, Central Switzerland.

$X_f \geqslant Y_f \geqslant Z_f$) is always contained in a plane parallel to the shear zone walls. The types of strain ellipsoid produced from these displacement fields are illustrated in the graphical plot of Fig. 4. Simple shear (Fig. 4, A) is clearly a plane strain ($e_2 = 0$). Heterogeneous volume reduction leads to progressive flattening ellipsoids (Fig. 4, B) and the combination leads to a deformation field in the apparent flattening sector of the diagram.

If the walls of the shear zone are themselves heterogeneously strained, then the displacement plans can be expressed mathematically as the same as (i) to (iii) above but with the addition (mathematically a matrix multiplication) of a homogeneous strain component inside and outside the shear zone, i.e.

(iv) homogeneous strain combined with simple shear (Fig. 3d);
(v) homogeneous strain combined with volume change (Fig. 3e);
(vi) homogeneous strain combined with simple shear and volume change (Fig. 3f)

With these three types the Y_f axis of the strain ellipsoids will have no specific relationship to the shear zone plane and all principal strain axes will have a variable orientation across a profile of the zone. The types of strain (i.e. apparent flattening or apparent constriction) have no general constraints, and all types are possible depending upon the orientations of the various 'componental' strains.

Although all six basic types are geometrically separable, it should be noted that their overall visual effect on marker surfaces crossing the shear zone is remarkably similar (see Fig. 3). This means that the field geologist has to be especially careful in avoiding jumping to premature conclusions as to the displacement field if he only observes deformed planar markers. In my experience natural shear zones accord very closely to these six models. Some geologists might object to the inclusion of models (ii) and (v) (Fig. 3b & e) which involve differential volume loss under the category of shear zones, but I think it is right to include them for two reasons. First their basic geometric boundary conditions accord with those of more 'orthodox' shear zones where shear is dominant (*S-bands*, Cobbold 1977a); second, their effects on oblique planar markers are geometrically very close to those of shear zones with differential shear displacement parallel to the zone walls. It will be shown later that the amount of volume change across a shear zone can be calculated using the displacement of initially plane markers. Deformation zones involving only volume loss are sometimes called *pressure solution zones* or *solution-seams* or *stripes* (Fig. 2e) or *P-bands* (Cobbold 1977a). These zones are usually deficient in certain mobile mineral species compared with their walls. In low to medium grade metamorphic environments, where such zones are common, quartz or calcite are usually removed from the rock leading to a proportional increase in relatively immobile components, such as clays, chlorite and micas. These changes in relative proportions of mineral species leads to a characteristic colour striping.

The deformation zones involving heterogeneous simple shear without differential volume change (types (i) and (iv), Fig. 3a & d) are commonly isochemical and the proportions of different mineral species across a zone profile is nearly constant. However, the mineral grain sizes and the rock fabric and texture do usually change with the strain variations across the zone.

The zones involving combinations of simple shear and volume change are usually variable in mineralogy, in mineral proportions and in texture and fabric (Fig. 2d).

SIMPLE SHEAR ZONES

The basic component in practically all shear zones is that of heterogeneous simple shear. It is therefore appropriate to investigate the geometric properties of this type of displacement, to establish how strains are related to displacement and how the structural features we see in deformed rocks within a shear zone can be related to displacement and strain.

A zone with heterogeneous simple shear can be considered to be made up of a number of infinitesimally small elements showing homogeneous simple shear. In such a small homogeneously strained element it is mathematically convenient to relate the x-coordinate direction parallel to the shear direction, and the z-axis normal to the plane of shear (xy) — see Fig. 5. If the top face of an initially cube element is displaced by a distance s, the shear strain γ (more exactly γ_{zx}) is related to the angular shear strain ψ produced by the deflection of the lines initially parallel to z such that

$$\gamma = \tan\psi \qquad (1)$$

$$\text{and so } s = z\tan\psi = z\gamma. \qquad (2)$$

The deformation matrix is then given by:

$$\begin{bmatrix} 1 & 0 & \gamma \\ 0 & 1 & 0 \\ 0 & 0 & 1 \end{bmatrix}. \qquad (3)$$

A circle of unit radius drawn on the xz face is deformed into a strain ellipse with principal semi-axis lengths along X_f of $1+e_1$ and along Z_f of $1+e_3$ (Fig. 6). The values of these strains are given by:

$$(1+e_1)^2 = \tfrac{1}{2}[2 + \gamma^2 + \gamma(\gamma^2+4)^{\frac{1}{2}}] \qquad (4)$$

$$e_2 = 0 \qquad (5)$$

$$(1+e_3)^2 = \tfrac{1}{2}[2 + \gamma^2 - \gamma(\gamma^2+4)^{\frac{1}{2}}]. \qquad (6)$$

The orientations θ' of these principal strains measured from the x coordinate direction is given by:

$$\tan 2\theta' = \frac{2}{\gamma}. \qquad (7)$$

These two directions originated in two other orthogonal directions θ in the unstrained state given by:

$$\tan 2\theta = \frac{-2}{\gamma}. \qquad (8)$$

The strain is clearly a rotational strain, the finite rotation ω can be derived from:

$$\tan \omega = \tan (\theta' - \theta) = \frac{2}{\gamma}. \tag{9}$$

Any passive plane marker is displaced by the shear such that, if its trace on the xz plane makes an initial angle α with the x-direction before deformation and an angle α' after deformation (Fig. 6), then

$$\cot \alpha' = \cot \alpha + \gamma. \tag{10}$$

The mathematical relationships refer to a special choice of coordinate reference frame such that x is parallel to the shear direction. It is sometimes more useful to refer to the displacements with the shear direction at some angle φ to the x-direction. For example one may be interested in computing the effects of subjecting an element to superposed shear zones at differing angles (we will discuss this problem later).

If the shear zone is oriented at an angle φ to the x-direction, then from the geometry shown in Fig. 7 an initial point (x,z) is displaced to a new position $(x_1 z_1)$ according to the displacement matrix:

$$\begin{bmatrix} 1 - \gamma \sin \varphi \cos \varphi & 0 & \gamma \cos^2\varphi \\ 0 & 1 & 0 \\ -\gamma \sin^2\varphi & 0 & 1 + \gamma \sin\varphi \cos \varphi \end{bmatrix}. \tag{11}$$

The values of the principal strains and rotations are identical to those of (4), (5), (6) and (9), but the orientation of the principal strains is given by

$$\tan 2\varphi' = \frac{2 + \gamma \tan 2\varphi}{\gamma + 2 \tan 2\varphi}. \tag{12}$$

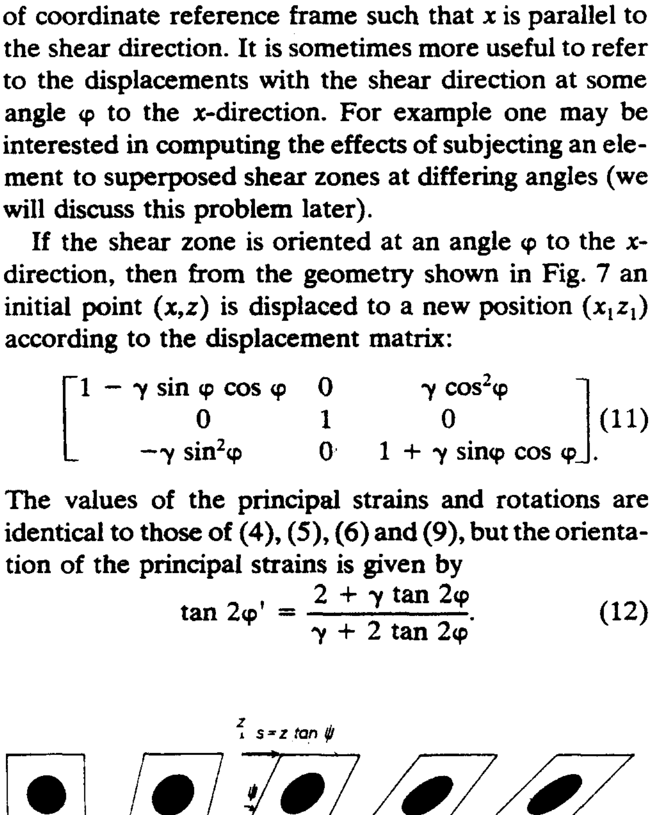

Fig. 5. The geometric features of simple shear, ψ, angular shear strain; s, displacement parallel to the x-axis.

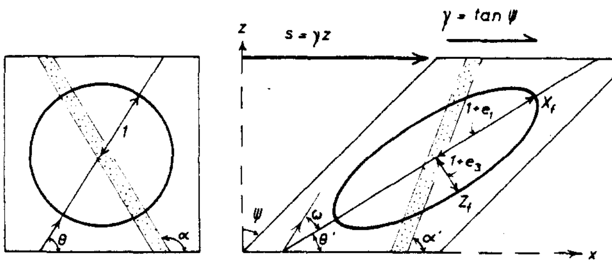

Fig. 6. The relation of the strain ellipse to shear in a simple shear system.

The positions of the principal strain axes for the first small increment of simple shear are from (7) oriented at 45° and 135° to the x-coordinate axis. The incremental strain axes X_i and Z_i are identically oriented and coincide with the principal strain rate axes. The principal

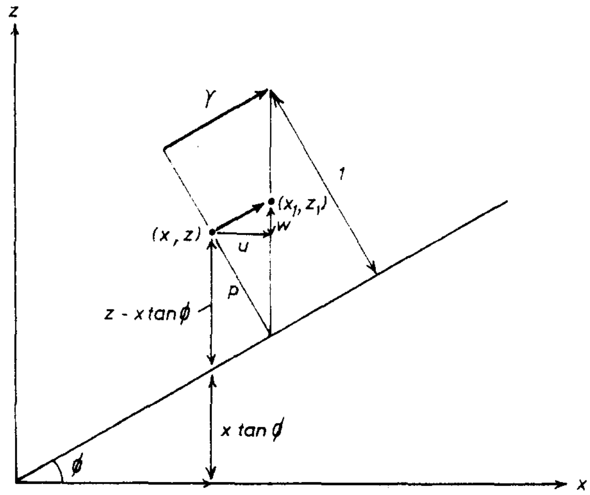

Fig. 7. Geometry of simple shear with shear oriented at an angle φ to the x coordinate axis.

strain rates $\dot{e}_1$ and $\dot{e}_3$ are related to the shearing strain rate $\dot{\gamma}_{zx}$ according to

$$\dot{e}_1 = -\dot{e}_3 = \frac{\dot{\gamma}_{zx}}{2}, \tag{13}$$

$$\dot{e}_2 = 0,$$

and the rate of rotation, or vorticity $\dot{\omega}$ is

$$\dot{\omega} = \dot{\gamma}. \tag{14}$$

During the first stages of deformation of an initially homogeneous isotropic body the principal axes of stress σ_1, σ_2 and σ_3 will coincide with the incremental strain axes X_i, Y_i and Z_i respectively, and the magnitudes of the strain rates will be some function of the magnitudes of the stresses. As deformation proceeds, however, it is very common for the deforming mass to become anisotropic as a result of the finite strains which build up with increasing values of shearing strain γ. During these mature stages of deformation, although the principal strain rate and incremental strain axes X_i and Z_i must remain at 45° and 135° to the x-direction because of geometric constraints of the process, the principal stress axes σ_1, and σ_3 will almost certainly be influenced by the increasing obliquity of the anisotropic fabric to these strain axes, and are therefore unlikely to coincide with the strain increment axes.

Fabrics produced by simple shear strain

As simple shear displacement gets larger, the angle θ' between the principal finite elongation X_f and the shear zone walls becomes progressively smaller (Fig. 8). In many naturally deformed rocks found in ductile shear zones, a statistically preferred orientation of the minerals is developed in this finite flattening plane, giving rise to schistosity or cleavage. Within this planar, tectonically induced fabric there is commonly a strain related linear orientation of the mineral components parallel to the finite greatest extension direction X_f on the schistosity plane. Progressive shearing leads to a progressive intensification of these linear fabrics and a change in

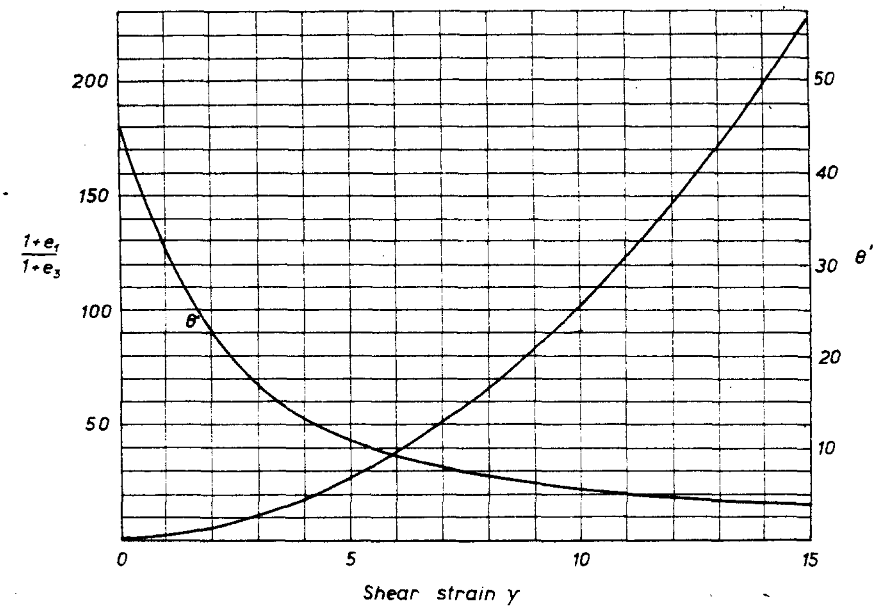

Fig. 8. Simple shear, values and orientations of the principal finite strains.

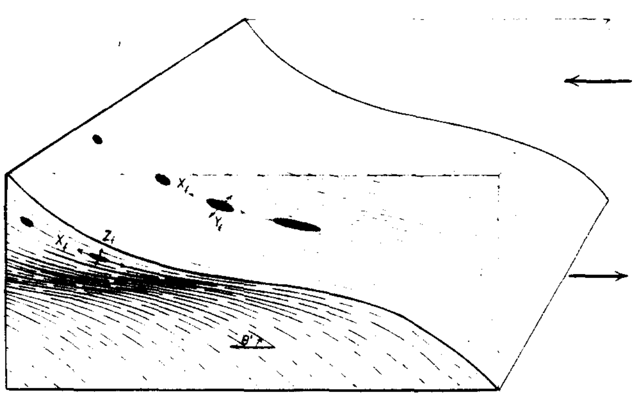

Fig. 9. Fabric in a ductile simple shear zone.

their orientation. Because ductile shear zones generally show a maximum displacement gradient in the zone centre (the gradient decreasing towards the margin), it follows that the tectonically induced planar fabrics of shear zones generally show a characteristic sigmoidal form as shown in Figs. 9 and 10.

Because the orientation of the $X_f Y_f$ surface with its coincident schistosity is a function of shear strain, it follows that the angle between schistosity and shear zone walls can be used to measure the shear zone parallel shear strain, and shape of the strain ellipsoid at that point. This technique, originally developed by Ramsay & Graham (1970), can be extended so as to integrate successive finite shear strains across a shear zone profile and, in so doing, to calculate the total differential displacement across a zone with heterogeneously developed shear strain (Fig. 11). The results of the application of this technique on a regional scale are often very striking. For example, Beach (1974) showed that the group of shear zones making up a large movement zone in the frontal part of the Precambrian Laxfordian orogenic belt of NW Scotland has a minimum displacement of 25 km, which can be resolved into a horizontal component of 18 km and a vertical component of 16 km.

The main problem of using this technique occurs where the shear displacement gradients are high. For example, angles between schistosity and shear zone wall of 5.7° and 2.9° imply a difference of displacement of 10γ and 20γ respectively. With such high displacement gradients (and high finite strains) very small observation errors can lead to gross errors in computing the total displacement across the shear zone.

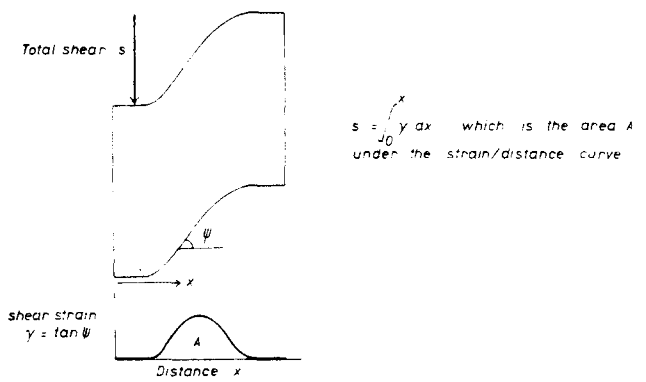

Fig. 11. Calculation of total displacement across a ductile shear zone.

Deformation of pre-existing planar features

It was pointed out above (equation 10 and Fig. 6) that pre-existing planar features have their orientation modified where they pass through a ductile shear zone. It should be stressed that the change of angle of equation 10 only applies to the trace of the original plane measured in the *xz* profile of the shear zone. Although it does not refer directly to the dihedral angle between two planes, the modification of such dihedral angles can be easily computed (Ramsay 1967, pp. 504–508). Where a set of sub-parallel planes crosses a shear zone with a varying displacement gradient profile, variations in the amount of local shear imposed on the layers sets up folding with a characteristic similar style (Fig. 12). The axes of these folds are controlled by the line of intersection of the initial plane structure and the xz plane of the zone. Their axial planes are parallel to the zone, and are located at positions dependent upon the local changes in shear gradient and the orientation of the plane before shearing (Ramsay 1967, pp. 508–509). Variations in orientation of the layers can be used to compute finite strain values at different positions in the zone (according to the relationships of equation 10), and can be used to determine the total shear across a zone. The practical application of this technique for calculating displacements has been shown in a beautiful study of basic dykes passing through shear zones along the Nagssugtoqidian orogenic front of west Greenland (Escher *et al.* 1975). Here it has been shown that shear zones have led to an average 66% crustal shortening of the deep level basement rocks of this orogen over a distance of about 100 km.

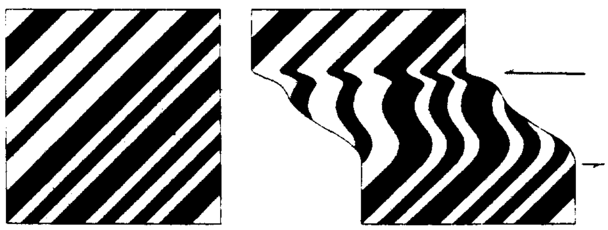

Fig. 12. Folds of 'similar' style produced by the shearing of passive layers.

The change in orientation of pre-existing planar features is accompanied by other geometric modifications. If there is no ductility contrast between the layer and its matrix it may either increase (Fig. 13a, i, ii) or decrease (Fig. 13b, i, ii) in thickness as a result of passive shearing. The conditions for increases or decreases in thickness are specified in Fig. 13. The change of thickness (t to t') is given by:

$$t' = \frac{\sin\alpha'}{\sin\alpha} t. \tag{15}$$

If the angular conditions are such that $\alpha > 90°$ and $\alpha' > 180° - \alpha$ the progressively sheared layer first thickens, then thins to its original width (where $\alpha' = 180° - \alpha$) and then subsequently becomes thinner than its original value. The reverse sequence — thinning followed by thickening — can never occur in progressive simple shear. If the layers undergoing shear are not passive, but show a competence contrast with their matrix, then mechanical instabilities are set up in the competent layer which lead to the formation of new structures. If the layer is shortened during deformation (equivalent to the passive layer undergoing thickening), buckle folds develop with wavelengths characteristic of the thickness of the competent layer, and the extent of the competence contrast (Fig. 13a, iii). The orientation of the axes of these folds depends upon the obliquity of the layer to the shear zone. It depends upon the direction of maximum shortening within the surface of the contracting competent layer and is not simply related to the principal displacement features of the shear system (as with the similar folds produced by passive layer deflection). For example, the fold axes will not generally form parallel to y or Y_f and they need not lie in the xy shear plane or the X_fY_f plane of the finite strain ellipsoid (Fig. 14).

If the competent layer is oriented in a position such that it becomes extended by the shearing, then pinch and swell or boudinage structure may be developed (Fig. 13b, iii). The necking directions of these boudins will be controlled by the maximum extension directions in the layer being sheared and will not in general, be related to the xy plane of the shear zone. In fact the two-dimensional strains within the deflected competent layer are likely to involve both extensions and contractions. Both buckle folding and boudinage then develop together, probably one of these being dominant over the other (Fig. 14).

One further possible complication that can develop in competent layers occurs where the initial orientation and value of shear lead to layer shortening followed by extension. Here we have the possibility of layers developing buckle folds, which subsequently become unfolded or boudinaged (Fig. 13c, iii).

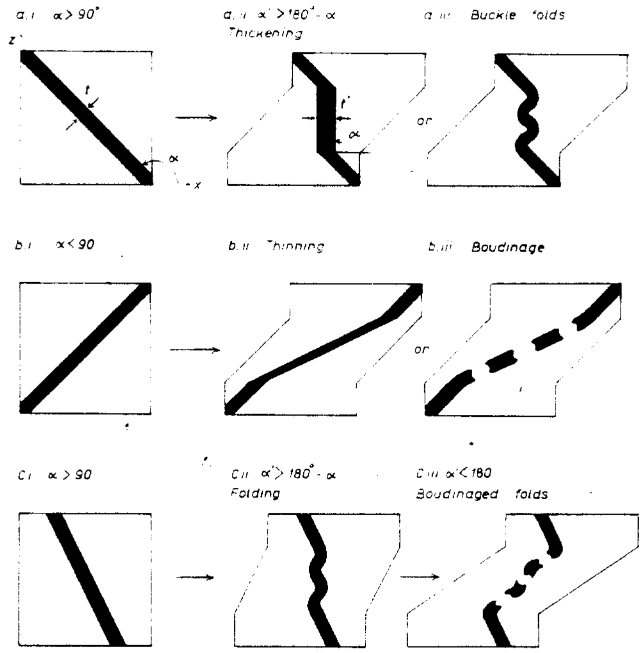

Fig. 13. Effects of shear zone deformation on competent layers.

Deformation of pre-existing linear features

Most pre-existing line elements (e.g. pre-shear zone fold axes) become deflected and take up new orientations in the shear zone. These lines come to lie closer to the direction of the shear (x) and move on a plane locus which connects their initial orientation with the x-direction (Fig. 15) (Weiss 1959, Ramsay 1960, 1967). In projection they move on a great circle locus (Fig. 15, p, p', p'' and q, q', q''). The only exceptions to this general rule are those lines which lie in the plane of the shear zone xy; these show no deflection (Fig. 15, r, r', r''). The axis of principal finite elongation X_f also moves

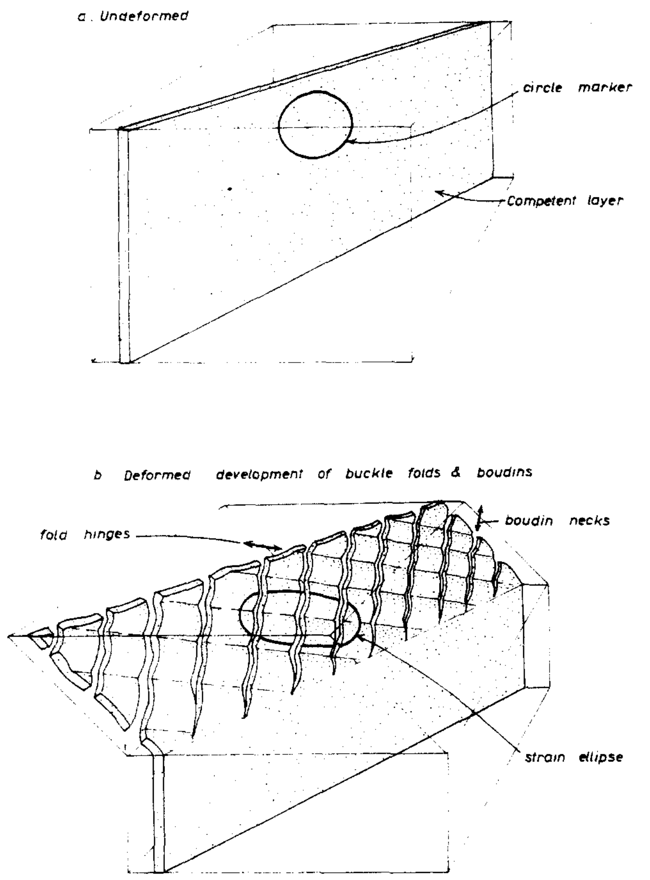

Fig. 14. Three-dimensional changes in a competent layer in a shear zone.

on the xz plane towards the x-direction (Fig. 15, X_f', X_f'').

The geometric effect of the drawing together of initially variably oriented linear directions towards the X_f direction is particularly striking at high shear strains. Particularly interesting is the effect described by Carreras *et al.* (1977) and Quinquis *et al.* (1978) where folds outside a shear zone showing slight variations in their axial plunges are deformed in the shear zone so that their axes show extreme variations in plunge (so called 'sheath folds'). The interlimb angles of these folds are drastically modified in the shear zone according to the principles discussed in the previous section and changes of fold shapes offer a method for computing shear strain values. This effect is shown diagrammatically in Fig. 16.

Terminations of shear zones

Ductile shear zones can, and in some cases do, come to a stop within the ductile environment. The boundary conditions for the ends of shear zones are much more complicated than for those of simple parallel sided zones with constant displacement profiles used to set up the six basic types described earlier. As far as I am aware there are no complete mathematical solutions for the possible finite strain and displacement variations where a shear zone terminates. However, one can proceed intuitively, and try and arrive at geometric resolutions which fit field observations and natural situations. There appear to be an unlimited range of possible models: Ramsay & Allison (1979) have suggested that this range has two

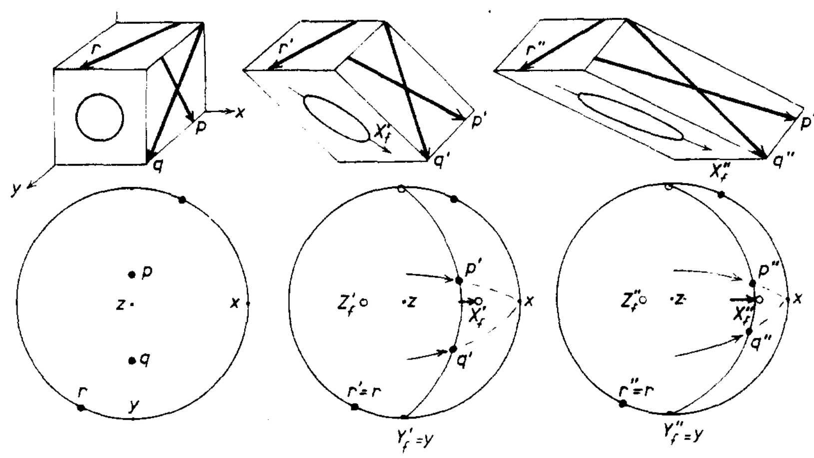

Fig. 15. Deformation of lineations in ductile shear zones.

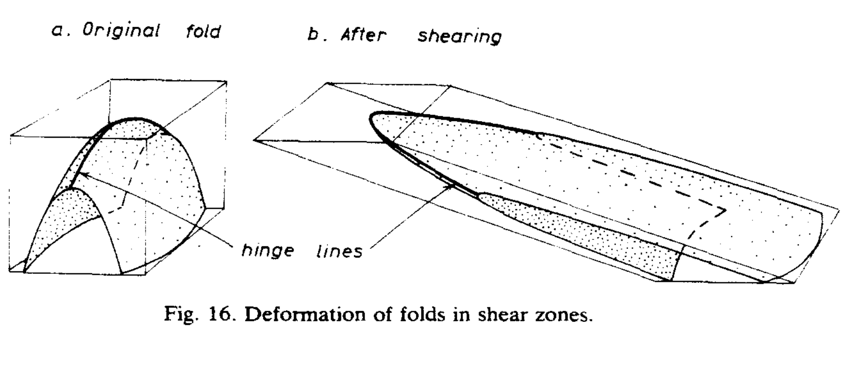

Fig. 16. Deformation of folds in shear zones.

end members (Fig. 17). One is a plane strain model, whereas the second is a solution where all displacements take place normal to the shear zone (in the y-direction). Both give rise to characteristic strain fields, and the non-plane strain model sets up constrictive and flattening deformations on either side of the shear zone tip. If the boundary deflections seen in the plane strain model are constrained, then there will be a tendency for the tips of right handed shear zones to bend and propagate in a clockwise sense with respect to the main shear zone, and left handed shear zones to propogate in an anticlockwise sense (Fig. 18). This effect could be the reason for the crossing or merging of shear zones of similar displacement sense that have been recorded in some regions.

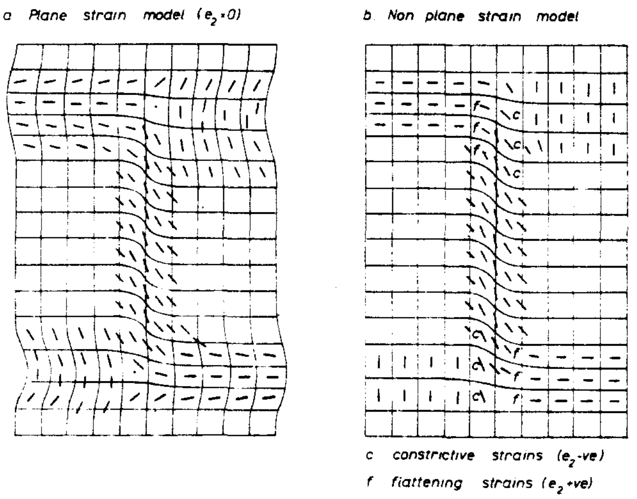

Fig. 17. Strain patterns at shear zone terminations.

GEOMETRIC FEATURES OF SHEAR ZONES INVOLVING VOLUME CHANGE

The geometry of simple shear zones of the type illustrated in Fig. 3(a) have been discussed in some detail because many of the structural characteristics of shear zones accord well with this model. However, this model is not a general one as it involves no volume change. We will now discuss the basic geometric features of more general models and establish ways the field geologist can separate the various componental strains and displacements.

Shear zones with undeformed walls (Figs. 3a, b & c)

The displacement fields in all of these types are most conveniently described in mathematical terms by a simple shear component (γ) followed by a volume change component (Δ) acting normal to the shear zone walls. The local displacement gradient matrix at any point in the zone can be described by the matrix

$$\begin{bmatrix} 1 & 0 & \gamma \\ 0 & 1 & 0 \\ 0 & 0 & 1+\Delta \end{bmatrix}. \tag{16}$$

The volume change component affects both the values and orientations of the principal strains

$$(1+e_1)^2 = \tfrac{1}{2}[1+\gamma^2+(1+\Delta)^2+ ((1+\gamma^2+(1+\Delta^2)^2-4(1+\Delta)^2)^{\frac{1}{2}}] \tag{17}$$

$$e_2 = 0 \tag{18}$$

$$(1+e_3)^2 = \tfrac{1}{2}[1+\gamma^2+(1+\Delta)^2- ((1+\gamma^2+(1+\Delta^2)^2-4(1+\Delta)^2)^{\frac{1}{2}}] \tag{19}$$

$$\tan 2\theta' = \frac{2\gamma(1+\Delta)}{1+\gamma^2-(1+\Delta)^2}. \tag{20}$$

In zones with varying shear and volume change the schistosity (X_fY_f plane) will be sigmoidally shaped, but the shape of these curved surfaces will not be a simple function of shear.

Passive line markers making an angle α with the shear zone walls are deflected in the zone to make a new angle α' such that

$$\cot\alpha' = \frac{\cot\alpha+\gamma}{1+\Delta}. \tag{21}$$

These relationships enable the shear and volumetric components to be separated. For example it is possible to compute γ and Δ from the deflections of two differently oriented deflected line (or plane trace) markers making initial angles of α and β and final angles of α' and β' (Fig. 19a), because from (21) it follows that:

$$\gamma = \frac{\cot\alpha\cot\beta' - \cot\beta\cot\alpha'}{\cot\alpha' - \cot\beta'} \tag{22}$$

and

$$1+\Delta = \frac{\cot\alpha - \cot\beta}{\cot\alpha' - \cot\beta'}. \tag{23}$$

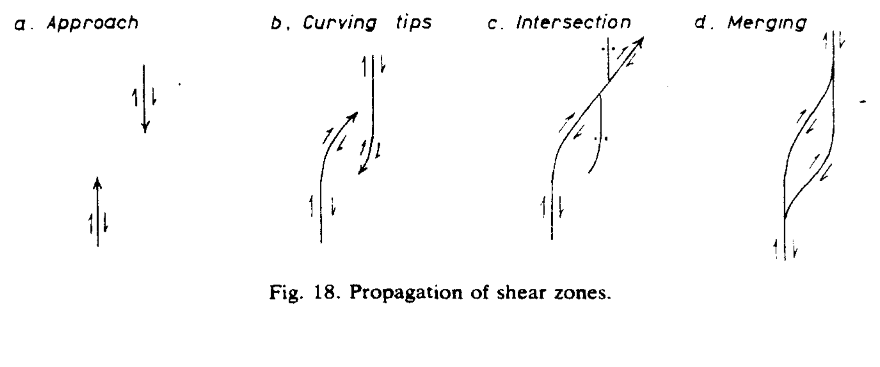

Fig. 18. Propagation of shear zones.

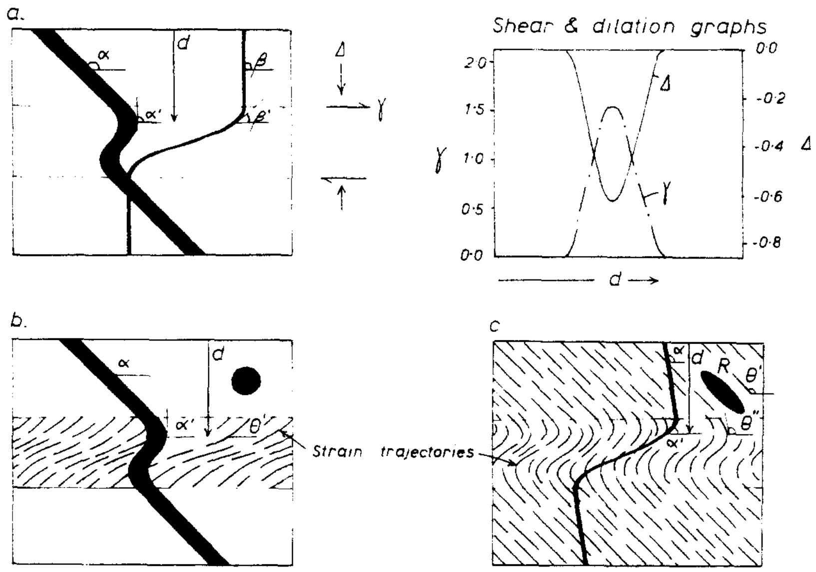

Fig. 19. Calculation of shear and dilation components in shear zones.

Another practical possibility for computing these two components occurs when a single line marker is deflected, and when the direction of principal strain axis θ' (schistosity trace on the shear zone profile) can be measured (Fig. 19b). Combining (20) and (21) we obtain a quadratic function for γ:

$$(\cot^2\alpha' - 2\cot\alpha'\cot 2\theta' - 1)\,\alpha^2 - 2\theta \cot\alpha\,(1 + \cot 2\theta'\cot\alpha)\gamma + (\cot^2\alpha' - \cot^2\alpha) = 0 \quad (24)$$

The two roots giving γ can then be used with (21) to obtain two corresponding solutions for the dilation. Both pairs of solutions are mathematically feasible, but it will be found that only one pair is geologically feasible, the other pair is spurious (e.g. where $1+\Delta$ is negative).

Shear zones with deformed walls

Shear zones with deformed walls represent the most general type of displacement field as illustrated in Fig. 3(f) (Ramsay & Graham 1970, Coward 1976, Cobbold 1977a). For analytical convenience such a zone may be considered as being made up of three successively imprinted components; the first a homogeneous strain (and homogeneous displacement gradient), the second a simple shear component, the third a volume change normal to the zone walls. In three dimensions the local displacement gradient is given by

$$\begin{bmatrix} l+r\gamma & m+s\gamma & n+t\gamma \\ 0 & p & q \\ r(1+\Delta) & s(1+\Delta) & t(1+\Delta) \end{bmatrix} \quad (25)$$

where 1, m . . . t represent the nine components of the homogeneous displacement, γ the simple shear component and Δ the volume change component. As pointed out previously, the principal strain orientations at different positions in the shear zone will have variable three-dimensional orientation and the strain trajectories across the zone will take complex curving forms. The two-dimensional geometry on a profile section of the zone (containing the x and z directions of the simple shear) can be expressed in a form which enables easier separation of the components:

$$\begin{bmatrix} a+b\gamma & b+d\gamma \\ b(1+\Delta) & d(1+\Delta) \end{bmatrix} \quad (26)$$

where a, $b = c$, d represent the 4 terms of the homogeneous displacement gradient matrix in the zone walls related to the shape (ellipticity R) and orientation (θ') of the strain ellipse in the wall rocks such that:

$$a = R^{\frac{1}{2}}\cos^2\theta' + R^{-\frac{1}{2}}\sin^2\theta', \quad (27)$$

$$b = (R^{\frac{1}{2}} - R^{-\frac{1}{2}})\sin\theta'\cos\theta', \quad (28)$$

$$d = R^{\frac{1}{2}}\sin^2\theta' + R^{-\frac{1}{2}}\cos^2\theta', \quad (29)$$

γ = simple shear zone component parallel to the x-axis,

Δ = volume change component parallel to the y-axis.

The orientation (θ'') of the principal strain axes inside the shear zone can now take on quite complex curved forms. Variations of γ and Δ can produce trajectory curves passing through angles exceeding 45° (i.e. not in accord with simple shear zone geometry) and which will link with principal strain directions in the matrix. At any point in the zone the orientations of principal strains is given by:

$$\tan 2\theta'' = \frac{2(1+\Delta)[b(a+d)+\gamma(b^2+d^2)]}{(a+b\gamma)^2+(b+d\gamma)^2-(b^2+d^2)(1+\Delta)^2}, \quad (30)$$

and the values of these strains in the surface of the profile are:

$$(1+e_1)^2 = \tfrac{1}{2}[a^2+b^2+2\gamma b(a+d)+(d^2+b^2)(\gamma^2+(1+\Delta)^2)+((a^2+b^2+2\gamma b(a+d)+(d^2+b^2)(\gamma^2+(1+\Delta)^2)^2-4(1+\Delta)^2(ad-b^2)^2)^{\frac{1}{2}}], \quad (31)$$

$$(1+e_2)^2 = \tfrac{1}{2}[a^2+b^2+2\gamma b(a+d)+(d^2+b^2)(\gamma^2+(1+\Delta)^2)-((a^2+b^2+2\gamma b(a+d)+(d^2+b^2)(\gamma^2+(1+\Delta)^2)^2-4(1+\Delta)^2(ad-b^2)^2)^{\frac{1}{2}}]. \quad (32)$$

The angular relationships of line markers outside and inside the shear zone are identical to those given in (21) and are independent of the values taken by the homogeneous strain component of the zone walls.

These general equations can be used with a computer to solve practical problems for separation of the shear zone component γ and dilation Δ. For example the solutions for two differently oriented lines outside (α and β) and inside (α' and β') the zone are identical to that of (22) and (23). Another important practical way of measuring these components arises when the ellipticity R and orientation θ' of the strain ellipse in the walls is known, the orientation of the strain ellipse at a point inside the zone is known (θ'') and when the deflections of a single line marker are available (α and α') (Fig. 19c). Then using (27), (28), (29) and (30) the shear strain component is derived from the following quadratic equation

$$\begin{aligned}&(b^2+d^2)\tan^2\alpha'(\tan 2\theta'(1+\tan^2\alpha')-2\tan\alpha)\gamma^2\\&+2\tan 2\theta'(\tan^2\alpha b(a+d)-\tan^2\alpha'\tan\alpha(b^2+d^2)\\&-2\tan\alpha\tan\alpha'(b(a+d)\tan\alpha+b^2+d^2))\gamma\\&+\tan 2\theta'((a^2+b^2)\tan^2\alpha-(b^2+d^2)\tan^2\alpha')\\&-2\tan\alpha\tan\alpha' b(a+d) = 0 \qquad (33)\end{aligned}$$

and the value of the volume change then obtained from (21). The two mathematically appropriate pairs of solutions are then inspected to discover the geologically significant result, as was discussed previously for the solution of (24).

A further method of separating volumetric and shear components arises when the ellipticity and orientation of the strain ellipse outside the zone, the ellipticity of the strain ellipse at a point inside the shear zone, and the deflections of a single line marker are all known. Equations (21) and (30) involve only the shear and volumetric components as unknowns and can therefore be used to obtain their values.

CONJUGATE SHEAR ZONES

Ductile shear zones of types (i), (iii), (iv) and (vi) generally occur in conjugate sets. A set of parallel shear zones is unable to change the overall shape of a rock mass into all possible new configurations, whereas deformation proceeded by two differently oriented sets of zones of the six basic types of shear zone can accommodate any overall regional shape change. One of the shear zone sets has a right handed shear displacement, the other is left handed. One of the most striking features of the angular relationships of the two sets of shears, which is in contrast to that of brittle shear zones (Anderson 1951), is that it is the obtuse angle (generally 90°–130°) between the shears which faces the greatest shortening direction of the system (Fig. 20b,i). At the intersection of the two conjugate sets one finds complex but not chaotic structures with much higher finite strains than are found in either of the two individual zones. The geometric features of the intersection generally indicate that one shear zone is later than the other and displaces it (e.g. Fig. 20b,i: the l-hand shear is later than the r-hand shear). Why this is so is a point worth discussion. I think it is connected with compatibility problems similar to those existing at the cross-over positions of brittle shear zones. The geometric problem is shown diagrammatically in Fig. 21. This shows the strains in the sector where the displacements of the two simple shears (of equal shear strain) are superposed. The strain state produced by shearing on zone (a) is followed by shearing on zone (b) (Fig. 21a) and is not the same as that where shearing on zone (a) follows that of zone (b) (Fig. 21b). The strain ellipses have the same ellipticity but their orientations differ. This may be verified mathematically for all angles of simple shear zone intersections using the displacement matrix of (11) first with values of γ, φ followed by $-\gamma$, $\varphi' = 180°-\varphi$, and then reversing the displacement order: the two total displacement matrices are different.

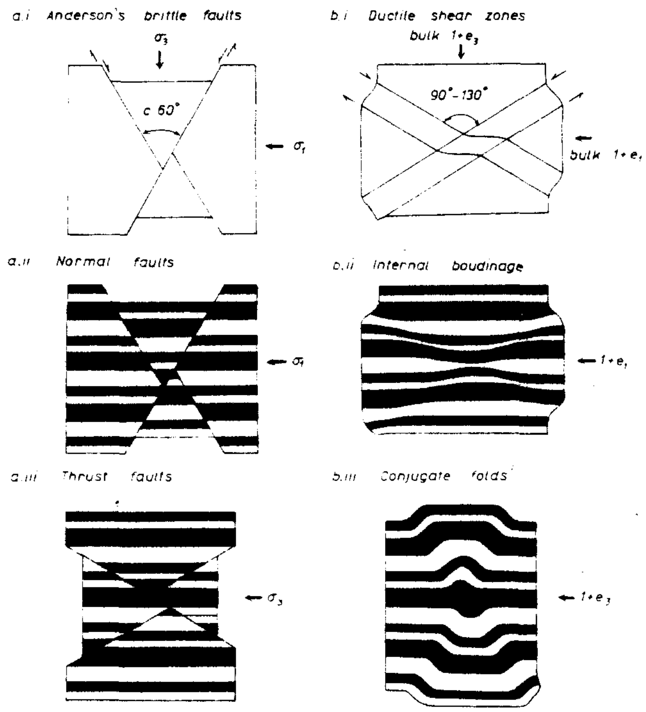

Fig. 20. Comparison of the geometric features of conjugate brittle and ductile shear zones.

The overall structural pattern of a region deformed by conjugate ductile shear zones is very characteristic: lozenge-shaped areas of relatively undeformed material are bounded by shear zones of right and left handed aspect. Such a pattern will be familiar to any geologist who has mapped 'basement' terrain for it is the normal deformation style. The dimensions of the lozenge-shaped areas can vary from the centimetric to the kilometric scale.

The geometric effect of developing conjugate ductile shear zones on a series of parallel passive layer marker horizons depends upon the orientation of this layering to the bulk strains produced by the conjugate shears.

If the layering is sub-perpendicular to the maximum

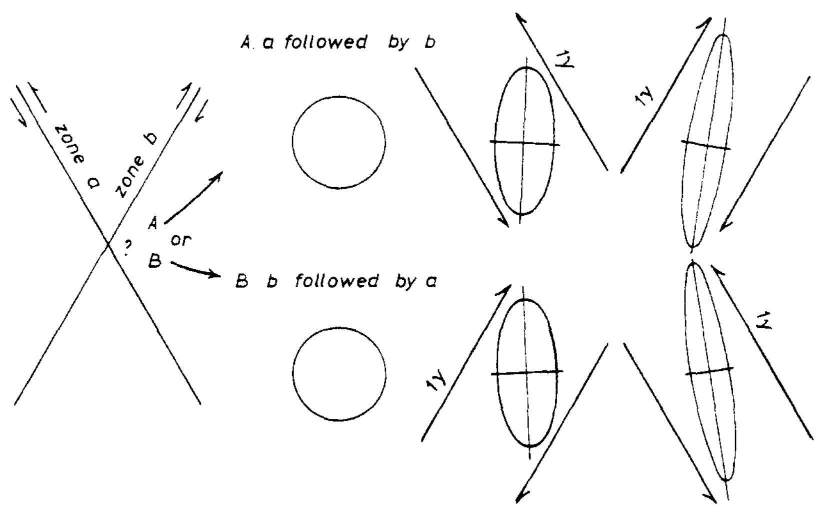

Fig. 21. Finite strains at the intersection of ductile shear zones.

bulk shortening of the whole mass the crossing shear zones give rise to a thinning of the layers, a feature which is especially noticeable where the layers pass through the intersection region of two conjugate shears (Fig. 20b,ii). The pronounced semi-symmetric thinning that occurs at the shear zone intersection has been termed *internal boudinage* (Cobbold *et al.* 1971). Internal boudinage, in contrast to normal boudinage, is not dependent upon competence contrasts between the boudinaged layer and its surrounding matrix, the neck zone being located only by the chance location of the intersecting shears. Internal boudinage is developed in rocks which are rheologically uniform or practically uniform. This structure might be considered to be the ductile equivalent of normal faulting (Fig. 20, cf. a,ii & b,ii).

If the layering is subnormal to the greatest extension of bulk strain then *conjugate folds* result. Such conjugate folds need not be genetically controlled by the layering, or by the thicknesses of individual beds within the multilayer packet although the planar anisotropy might be the instigator of the shear zones (Cobbold *et al.* 1971). This conjugate fold structure might be considered as the ductile homologue of brittle shear zone thrust faults (Fig. 20, cf. a,ii & b,ii).

REGIONAL DEVELOPMENT OF SHEAR ZONES: RELATIONSHIPS BETWEEN DEEP LEVEL DUCTILE ZONES AND HIGH LEVEL BRITTLE ZONES

Of particular interest to structural geologists is the behaviour of regional shear zones which pass from ductile types at deep levels to brittle types at higher crustal levels. This problem is of major importance in discussions of basement-cover relations in orogenic belts and in zones of regional crustal extension.

Contraction zones

Most, if not all, orogenic belts show an overall shortening of the sedimentary sheets of cover strata by means of thrusting and nappe gliding. These cover strata are commonly of continental shelf facies known to have been laid down on crystalline continental type basement. Where this basement is exposed in the orogenic zone it is usually seen to contain ductile shear zones. The relationships of deep level ductile shear zones with higher level thrust that accord best with my own experience are shown schematically in Fig. 22. The shortening of the basement leads to an uplift of the internal part as a result of the crustal thickening. The ductile shear zones pass upwards across the basement-cover unconformity, and the ductile shear that is common to both basement and cover here accounts for many of the changes in angular relationships between the two series of rocks. At higher levels the ductile shear zone is transformed into a brittle–ductile zone with the upper side of the zone showing less ductile features than the lower. At still higher levels the internal deformation of the cover sediments becomes less marked and is mostly related to displacements associated with flexural slip movements in incompetent layers within the succession. The cover shortening that is not taken up by these folds is accomplished by low angle thrusts passing into strata-guided 'glide sheets' (Fig. 23). The thrusts below the glide sheets move to progressively higher stratigraphic levels outwards from the orogenic zone, making high angle steps where they cut across competent layers. The brittle shear zone eventually reaches the surface at the thrust toe.

Extension zones

The structural features of the upper crustal levels are quite well known from studies of graben and rift systems, but the structural relationships of these high level phenomena to those of the underlying basement are less well known. Moderately to steeply inclined normal faults (45° to 60°) predominate at the high levels, the fault plane geometry being guided by strata competence, being steepest in the most competent layers (Fig. 24). Normal fault displacements over the irregular fault surfaces lead to geometric features related to compatibility

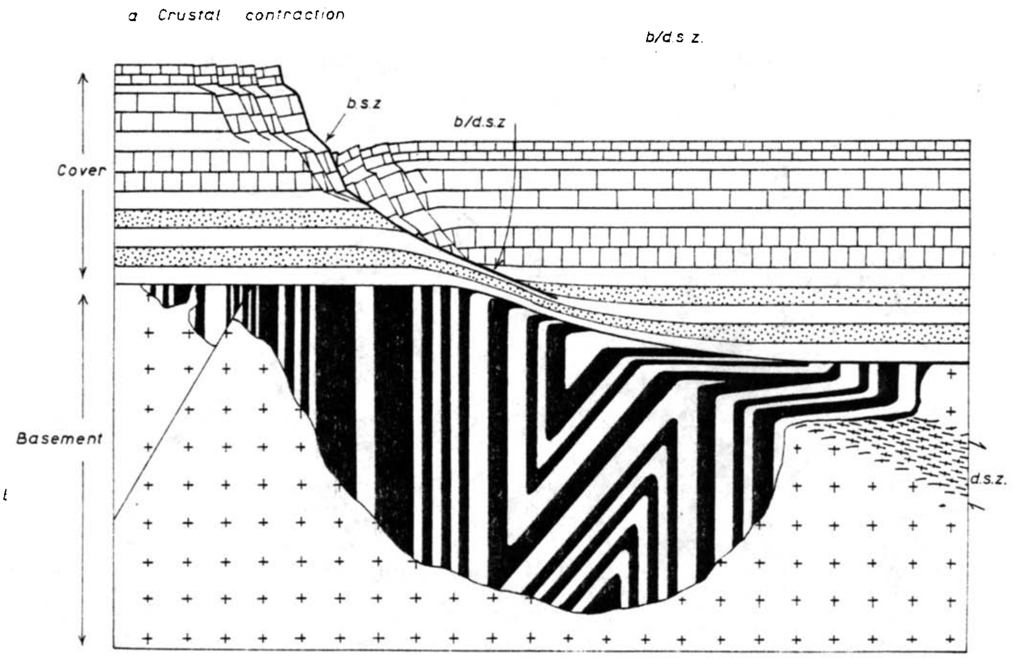

Fig. 22. Relationships of brittle and ductile shear zones: crustal contraction.

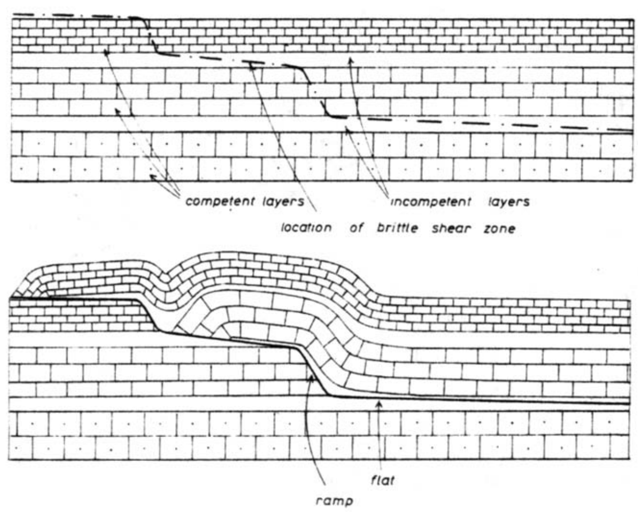

Fig. 23. Fold and fault geometry — high level nappes.

problems in the same way that geometric problems arise from pushing low angle thrust sheets across their underlying ramps and flats (Fig. 23).

At deeper levels the rheological contrasts of the cover layers become less marked, and we pass through a lower angle brittle–ductile shear zone transition into conjugate low angle ductile shear zones. These shear zones enable the deep crustal levels to extend: they can give rise to internal boudinage (Davis & Coney 1979) or to conjugate folding of the layering in the basement depending upon the orientation of this layering. Conjugate pairing of the shear zones is necessary for a complete horst-graben tectonic pattern at higher levels. Basement-cover angular unconformities will be geometrically modified where crossed by ductile shear zones (see Fig. 24).

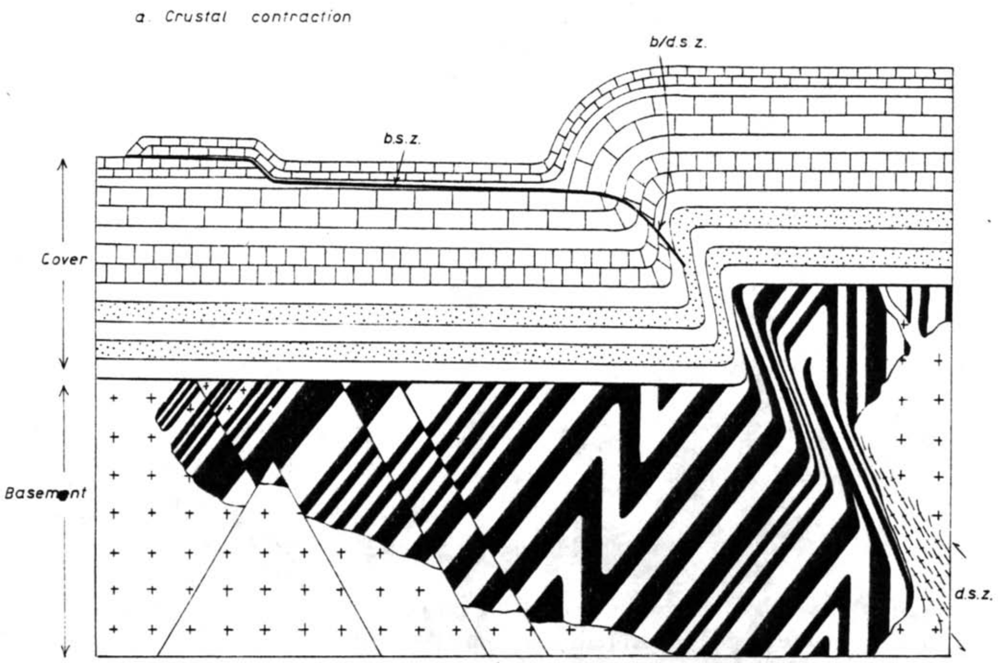

Fig. 22. Relationships of brittle and ductile shear zones: crustal contraction.

REFERENCES

Anderson, E. M. 1951. *The Dynamics of Faulting*. Oliver & Boyd, Edinburgh.

Beach, A. 1974. The measurement and significance of displacements on Laxfordian shear zones, North-west Scotland. *Proc. Geol. Ass.* **85**, 13-21.

Carreras, J., Estrada, A. & White, S. 1977. The effects of folding on the c-axis fabrics of a quartz mylonite. *Tectonophysics* **39**, 3–24.

Cobbold, P. R. 1976. Fold shapes as functions of progressive strain. *Phil. Trans. R. Soc.* **A283**, 129–138.

Cobbold, P. R. 1977a. Description and origin of banded deformation structures. I. Regional strain, local perturbations, and deformation bands. *Can. J. Earth Sci.* **14**, 1721–1731.

Cobbold, P. R. 1977b. Description and origin of banded deformation structure. II. Rheology and the growth of banded perturbations. *Can. J. Earth Sci.* **14**, 2510–2523.

Cobbold, P. R., Cosgrove, J. W. & Summers, J. M. 1971. Development of internal structure in deformed anisotropic rocks. *Tectonophysics* **12**, 23–53.

Coward, M. P. 1976. Strain within ductile shear zones. *Tectonophysics* **34**, 181–197.

Davis, G. H. & Coney, P. J. 1979. Geologic development of the Cordilleran metamorphic core complexes. *Geology* **7**, 120–124.

Escher, A., Escher, J. C. & Watterson, J. 1975. The reorientation of the Kangamiut dyke swarm, West Greenland. *Can. J. Earth Sci.* **12**, 158–173.

Quinquis, H., Audren, C. L., Brun, J. P. & Cobbold, P. R. 1978. Intense progressive shear in the Ile de Groix blueschists. *Nature, Lond.* **273**, 43–45.

Ramsay, J. G. 1960. The deformation of lineations in areas of repeated folding. *J. Geol.* **68**, 75–93.

Ramsay, J. G. 1967. *Folding and Fracturing of Rocks*. McGraw-Hill, New York.

Ramsay, J. G. & Graham, R. H. 1970. Strain variation in shear belts. *Can. J. Earth Sci.* **7**, 786–813.

Ramsay, J. G. & Allison, I. in press. Structural analysis of shear zones in a deformed granite from the Pennine zone, Swiss Alps. *Schweiz. miner. petrogr. Mitt.*

Teall, J. J. H. 1885. The metamorphosis of dolerite into hornblende schist. *Q. Jl geol. Soc. Lond.* **41**, 133–145.